

# CRACK GROWTH IN ELASTIC-PLASTIC MATERIALS WITH STRAIN GRADIENT EFFECTS

E. Radi, M. Gei

*Dipartimento di Scienze e Metodi dell'Ingegneria - Università di Modena e Reggio Emilia -  
Viale Allegri 13, 42100 Reggio Emilia*

## ABSTRACT

Strain-gradient effects on the asymptotic near-tip stress and velocity fields of a crack propagating steadily and quasi-statically in an elastic-plastic material displaying linear hardening are highlighted. The flow theory version of couple stress plasticity is adopted for the constitutive description of the material. Under mode I crack propagation a substantial increase of the stress singularity is observed and, thus, of the traction level ahead of the crack-tip, whereas an increase in the shear traction ahead of the crack-tip is noticed under mode II loading conditions.

## SOMMARIO

Lo stato tensionale all'apice di una frattura che si propaga in un materiale duttile è fortemente condizionato dalla presenza di "strain gradient" dovuti a dislocazioni geometricamente necessarie. In questa nota si studia l'entità di questa influenza adottando la teoria della plasticità "couple stress" recentemente proposta per lo studio degli effetti dimensionali nei metalli. L'incremento di singolarità è evidente soprattutto in modo I, mentre in modo II si nota un aumento del valore delle tensioni tangenziali davanti all'apice.

## INTRODUCTION

Due to strain gradients which arise for non-uniform deformations, ductile materials display size effect when deformed at the micron scale, as confirmed in a large number of experimental tests (see [1] for a review of the subject). However, conventional plasticity theories are unable to explain this phenomenon. Similar remarks apply to fracture mechanics. Elssner et al. [2] showed that when the crack growth mechanism involves cleavage or decohesion at the atomic scale, the measured stress level is of the order of 10 times the tensile yield stress, a value sensibly high compared to the classical predictions [3, 4]. Therefore, for refined analyses at the micron scale, it becomes necessary to adopt enhanced constitutive models, which take into account the microstructure of the material and the presence of strain gradients.

In this note, near-tip fields for plane strain mode I and mode II crack growth are calculated by employing the couple stress plasticity proposed by Fleck and Hutchinson [5]. This model is a generalization of the classical  $J_2$ -flow theory obtained by adding the effects of strain rotation gradients, which are significant within a zone of radius  $\ell$ ,

where  $\ell$  is a material characteristic length entering in the formulation (typically of the order of few microns for ductile solids). Outside of this area the strain gradients become negligible and the adopted constitutive model reduces to the conventional flow theory.

## CRACK PROPAGATION PROBLEM

The problem of a plane crack propagating at constant velocity  $V$  along a rectilinear path in an infinite medium is considered. A cylindrical co-ordinate system  $(r, \theta, x_3)$  moving with the crack-tip towards the  $\theta = 0$  direction is considered, where the  $x_3$ -axis coincides with the straight crack front. The condition of steady-state crack propagation yields the following time derivative rule, which holds for any scalar function  $\phi$

$$\dot{\phi} = \frac{V}{r} (\phi_{,\theta} \sin\theta - r \phi_{,r} \cos\theta), \quad (1)$$

where  $r$  and  $\theta$  are the polar coordinates in the plane orthogonal to the  $x_3$ -axis.

The considered constitutive model refers to the flow theory version of the strain gradient plasticity presented by Fleck and Hutchinson [5]. This model fits within the general framework of couple stress theory and involves a single material length scale  $\ell$ , specifying the order of non-uniform deformation at which the effects of strain gradients become significant, and thus is generally *small* (about 4  $\mu\text{m}$  for copper and 6  $\mu\text{m}$  for nickel).

According to the couple stress model [6, 7], a surface element of a body with unit area can transmit a force traction vector  $\mathbf{t}$  and a couple stress traction vector  $\mathbf{q}$ . These surface forces  $\mathbf{t}$  and  $\mathbf{q}$  can be expressed in terms of the non-symmetrical Cauchy stress tensor  $\boldsymbol{\zeta}$  and of the couple stress tensor  $\boldsymbol{\mu}$  as

$$\mathbf{t} = \boldsymbol{\zeta}^T \mathbf{n} + \nabla \mu_{nn} \times \mathbf{n} / 2, \quad \mathbf{q} = (\mathbf{I} - \mathbf{n} \otimes \mathbf{n}) \boldsymbol{\mu}^T \mathbf{n}. \quad (2)$$

In the following the Cauchy stress  $\boldsymbol{\zeta}$  will be decomposed into the symmetric part  $\boldsymbol{\sigma}$  and the skew-symmetric part  $\boldsymbol{\tau}$ .

For a plane problem, the non-vanishing in-plane stress and couple stress components in polar coordinates are  $\sigma_{rr}$ ,  $\sigma_{\theta\theta}$ ,  $\sigma_{\theta r}$ ,  $\tau_{\theta r}$ ,  $\mu_{r3}$  and  $\mu_{\theta 3}$ , with  $\sigma_{r\theta} = \sigma_{\theta r}$  and  $\tau_{r\theta} = -\tau_{\theta r}$ . Accordingly, the in-plane strain and deformation curvature components are  $\varepsilon_{rr}$ ,  $\varepsilon_{\theta\theta}$ ,  $\varepsilon_{\theta r}$ ,  $\chi_{3r}$ , and  $\chi_{3\theta}$ , with  $\varepsilon_{r\theta} = \varepsilon_{\theta r}$ . Moreover, the condition  $\varepsilon_{33} = 0$  must be imposed for plane strain problems and the boundary conditions (2) result in

$$\sigma_{\theta r} + \tau_{\theta r} = \sigma_{\theta\theta} = 0, \quad \mu_{\theta 3} = 0. \quad (3)$$

With respect to a polar coordinate system, the equilibrium equations are

$$\begin{aligned} r \sigma_{rr,r} + \sigma_{\theta r,\theta} + \sigma_{rr} - \sigma_{\theta\theta} + \tau_{\theta r,\theta} &= 0, \\ r (\sigma_{\theta r,r} - \tau_{\theta r,r}) + \sigma_{\theta\theta,\theta} + 2 \sigma_{\theta r} &= 0, \\ r (\mu_{r3,r} - 2 \tau_{\theta r}) + \mu_{\theta 3,\theta} + \mu_{r3} &= 0, \end{aligned} \quad (4)$$

and kinematic compatibility requires that

$$\dot{\varepsilon}_{rr} = v_{r,r}, \quad r \dot{\varepsilon}_{\theta\theta} = v_r + v_{\theta,\theta}, \quad 2 r \dot{\varepsilon}_{r\theta} = v_{r,\theta} - v_\theta + r v_{\theta,r}, \quad (5)$$

$$r \dot{\chi}_{3r} = r \dot{\epsilon}_{r0,r} + 2 \dot{\epsilon}_{r0} - \dot{\epsilon}_{rr,0}, \quad r \dot{\chi}_{30} = r \dot{\epsilon}_{00,r} + \dot{\epsilon}_{00} - \dot{\epsilon}_{rr} - \dot{\epsilon}_{r0,0}, \quad (6)$$

$$\dot{\chi}_{3r,0} - (r \dot{\chi}_{30})_{,r} = 0. \quad (7)$$

Within the context of small deformations incremental theory, the total strain rate  $\dot{\epsilon}$  is the sum of elastic  $\dot{\epsilon}^e$  and plastic  $\dot{\epsilon}^p$  parts. Similarly, the total deformation curvature rate  $\dot{\chi}$  is the sum of elastic  $\dot{\chi}^e$  and plastic  $\dot{\chi}^p$  contributions. Both elastic parts are related to stress and couple stress rates through the incremental relations

$$\dot{\epsilon}^e = \frac{1}{E} [(1 + \nu) \dot{\sigma} - \nu (\text{tr} \dot{\sigma}) \mathbf{I}], \quad \dot{\chi}^{eT} = \frac{1 + \nu}{E \ell_e^2} \dot{\mu}, \quad (8)$$

where  $E$  denotes the elastic Young modulus,  $\nu$  the Poisson ratio and  $\ell_e$  is the elastic length scale introduced in [5] in order to partition the deformation curvature rate tensor into its elastic part  $\dot{\chi}^e$  and plastic part  $\dot{\chi}^p$ , being  $\ell_e < \ell$ . It is worth noting that, within the couple stress theory  $\mu$ ,  $\chi$ ,  $\chi^e$ , and  $\chi^p$  are purely deviatoric tensors.

The fundamental relationships of the constitutive model are briefly summarized below.

- Yield condition

$$f(\Sigma, Y) = \Sigma - Y = 0, \quad (9)$$

where  $\Sigma$  is the overall effective stress, defined as

$$\Sigma^2 = 3/2 (\sigma^{\text{dev}} \cdot \sigma^{\text{dev}} + \ell^{-2} \mu \cdot \mu), \quad (10)$$

and  $Y$  denotes the uniaxial flow stress defining isotropic hardening behaviour.

- Flow rule

$$\dot{\epsilon}^p = \Lambda \frac{\partial f}{\partial \sigma} = \frac{3}{2 \Sigma} \sigma^{\text{dev}}, \quad \dot{\chi}^{pT} = \Lambda \frac{\partial f}{\partial \mu} = \frac{3}{2 \Sigma \ell^2} \mu, \quad (11)$$

where  $\Lambda$  is the plastic multiplier.

- Linear isotropic hardening rule

$$\dot{Y} = \Lambda H, \quad (12)$$

where  $H = \alpha E / (1 - \alpha)$  is the hardening modulus, and  $\alpha = E_t / E$  ( $0 < \alpha < 1$ ) is the ratio between the tangent modulus and the elastic Young modulus for a bilinear stress-strain curve obtained by a uniaxial tension test.

- Prager consistency condition

$$\dot{f} = 0, \text{ or equivalently } \dot{\Sigma} = \dot{Y},$$

which gives the non-negative plastic multiplier  $\Lambda$  as

$$\Lambda = \begin{cases} \langle \dot{\Sigma} \rangle / H & \text{if } f(\Sigma, Y) = 0 \\ 0 & \text{if } f(\Sigma, Y) < 0, \end{cases} \quad (13)$$

where  $\langle \cdot \rangle$  denotes the MacAuley brackets and

$$\dot{\Sigma} = \frac{3}{2 \Sigma} (\sigma^{\text{dev}} \cdot \dot{\sigma} + \ell^{-2} \mu \cdot \dot{\mu}). \quad (14)$$

From (8) the elastic-plastic incremental constitutive equations for the stress and couple stress tensors,  $\sigma$  and  $\mu$ , turn out to be

$$\dot{\boldsymbol{\varepsilon}} = \frac{1}{E} [(1 + \nu)\dot{\boldsymbol{\sigma}} - \nu(\text{tr}\dot{\boldsymbol{\sigma}})\mathbf{I}] + \frac{3}{2\Sigma} \Lambda \boldsymbol{\sigma}^{\text{dev}}, \quad (15)$$

$$\ell^2 \dot{\boldsymbol{\chi}}^T = \frac{1+\nu}{E \xi^2} \dot{\boldsymbol{\mu}} + \frac{3}{2\Sigma} \Lambda \boldsymbol{\mu}, \quad (16)$$

where  $\xi = \ell_e/\ell < 1$  is a non-dimensional parameter. Equations (15)-(16) hold when the stresses and couple stresses satisfy the yield condition (9). Otherwise, the incremental constitutive relationship reduces to the couple stress isotropic elasticity [6, 7], recovered when  $\Lambda = 0$ . Note that strain gradient effects occur also for a purely elastic response. However, their magnitude may be made arbitrarily small by choosing a sufficiently small  $\xi$  ratio. Finally, it can be observed that the resulting constitutive equations (15)-(16) represent a generalization of the widely used  $J_2$ -flow theory of plasticity, and reduce to that model when the strain gradients are vanishing small.

### ASYMPTOTIC CRACK-TIP FIELDS

Equations (4)-(7) together with the constitutive incremental equations (12), (15) and (16) form a system of first order PDEs which governs the problem of the crack propagation. The solution is sought in separable variable form, which corresponds to the most singular term in the asymptotic expansion of near crack-tip fields. A qualitative analysis shows that the velocity, stress and couple stress crack-tip fields admit the following asymptotic representations

$$\begin{aligned} \mathbf{v}(\mathbf{r}, \theta) &= -\frac{V}{s} \left(\frac{\mathbf{r}}{R}\right)^s \mathbf{w}(\theta), & \boldsymbol{\sigma}(\mathbf{r}, \theta) &= E \left(\frac{\mathbf{r}}{R}\right)^s \mathbf{S}(\theta), & \tau_{\theta r}(\mathbf{r}, \theta) &= E \left(\frac{\mathbf{r}}{R}\right)^s T_{\theta r}(\theta), \\ \boldsymbol{\mu}(\mathbf{r}, \theta) &= E \ell \left[ \left(\frac{\mathbf{r}}{B}\right)^t \mathbf{m}(\theta) + \dots + \frac{\mathbf{r}}{\ell} \left(\frac{\mathbf{r}}{R}\right)^s \mathbf{n}(\theta) \right] \otimes \mathbf{e}_3, \end{aligned} \quad (17)$$

where  $R$  and  $B$  denote two characteristic lengths which define the amplitude of the leading order term of the stress and couple stress fields. In particular,  $B$  is assumed to coincide with  $R$  when  $t = s$ , so that, in this case, both the leading order terms of the stress and couple stress fields are defined within a single amplitude factor.

According to representations (17) of the stress and couple stress crack-tip fields the overall effective stress and flow stress fields assume the following form

$$\Sigma(\mathbf{r}, \theta) = E \left(\frac{\mathbf{r}}{P}\right)^p \Gamma(\theta), \quad Y(\mathbf{r}, \theta) = E \left(\frac{\mathbf{r}}{P}\right)^p \gamma(\theta), \quad (18)$$

where  $p = \min\{s, t\}$ ,  $P = B$  if  $t < s$  or  $P = R$  if  $t \geq s$  and the function  $\Gamma$  follows from (10) and (17)<sub>2,4</sub> as

$$\Gamma^2 = \frac{3}{2} \begin{cases} \mathbf{m} \cdot \mathbf{m} & \text{if } t < s \\ \mathbf{S}^D \cdot \mathbf{S}^D + \mathbf{m} \cdot \mathbf{m} & \text{if } t = s \\ \mathbf{S}^D \cdot \mathbf{S}^D & \text{if } t > s. \end{cases} \quad (19)$$

By using the steady-state derivative (1), the rates of the fields  $\boldsymbol{\sigma}$ ,  $\boldsymbol{\mu}$  and  $Y$  in (17)<sub>2,4</sub> and (18) can be written as

$$\begin{aligned}
\dot{\mathbf{c}}(r, \theta) &= E \frac{V}{r} \left( \frac{r}{R} \right)^s \boldsymbol{\Sigma}(\theta), \\
\dot{\boldsymbol{\mu}}(r, \theta) &= E V \left[ \frac{\ell}{r} \left( \frac{r}{B} \right)^t \mathbf{h}(\theta) + \dots + \left( \frac{r}{R} \right)^s \mathbf{k}(\theta) \right] \otimes \mathbf{e}_3, \\
\dot{Y}(r, \theta) &= E \frac{V}{r} \left( \frac{r}{P} \right)^p \kappa(\theta).
\end{aligned} \tag{20}$$

The constitutive relations (15) and (16) imply that the strain and deformation curvature rates must have the same radial dependence assumed for the stress and couple stress rates in (20), respectively. Therefore, the following asymptotic representations are assumed for the strain and deformation curvature rates

$$\begin{aligned}
\dot{\boldsymbol{\varepsilon}}(r, \theta) &= \frac{V}{r} \left( \frac{r}{R} \right)^s \mathbf{D}(\theta), \\
\dot{\boldsymbol{\chi}}(r, \theta) &= \frac{V}{\ell^2} \mathbf{e}_3 \otimes \left[ \frac{\ell}{r} \left( \frac{r}{B} \right)^t \mathbf{x}(\theta) + \dots + \left( \frac{r}{R} \right)^s \mathbf{y}(\theta) \right],
\end{aligned} \tag{21}$$

so that for  $t > s - 1$  the right hand sides of the compatibility equations (6) are more singular than the left hand sides. It follows that the dominant strain rate field turns out to be irrotational, as occurs for the problem of a stationary crack [8, 9], although the leading order term of the deformation curvature is not vanishing.

By contrast with the approach of Xia and Hutchinson [8] and Huang et al. [9] for the problem of a stationary crack, in the present analysis the leading order term of the deformation curvature rate is not vanishing, but couples with higher order terms of the strain rate and velocity fields, which behave as  $r^t$  and  $r^{t+1}$  as  $r \rightarrow 0$ , respectively.

It is worth noting that the solution of the homogeneous asymptotic problem can be determined up to the amplitude factors  $B$  and  $R$ , which depend on far-field loading and specimen geometry and can be estimated by matching with the far-field conditions. Nevertheless, the asymptotic analysis can capture the strength of the singularity of the stress and couple stress fields, namely  $s$  and  $t$ , and the variation of the angular functions normalized by the condition  $S_{\theta\theta}(0) = 1$  under mode I, or  $S_{\theta r}(0) = 1$  under mode II. Moreover, for  $t \neq s$  the additional normalization condition  $m_\theta(0) = 1$  under mode I, or  $m_r(0) = 1$  under mode II, must be considered for the leading order couple stress fields. The formulation of the solving eigenvalue problem is detailed in [10]. Its solution holds for  $r < \ell$ , even if the asymptotic analysis has been extended to the second order terms of the couple stress and deformation curvature fields. Indeed, for  $r > \ell$  a switch between the leading and higher order terms may occur in the asymptotic expansions (17)<sub>4</sub> and (21)<sub>2</sub>, which implies a transition towards a stress dominated solution at a sufficiently large distance from the crack-tip. In any case, strain gradient effects are expected to be significant within a zone of radius larger than  $\ell$  [8].

As a further outcome, the angles which define the boundary between plastic and elastic sectors ( $\theta_1$  and  $\theta_2$ ) are calculated. In particular, considering only the interval  $0 < \theta < \pi$ ,

if elastic unloading occurs, the zone with  $\theta < \theta_1$  is plastic, that with  $\theta_1 < \theta < \theta_2$  is an elastic sector where  $f(\Sigma, Y) < 0$  (cf. eq. 8), and that with  $\theta_2 < \theta < \pi$  is a reloading plastic sector adjacent to the crack flank.

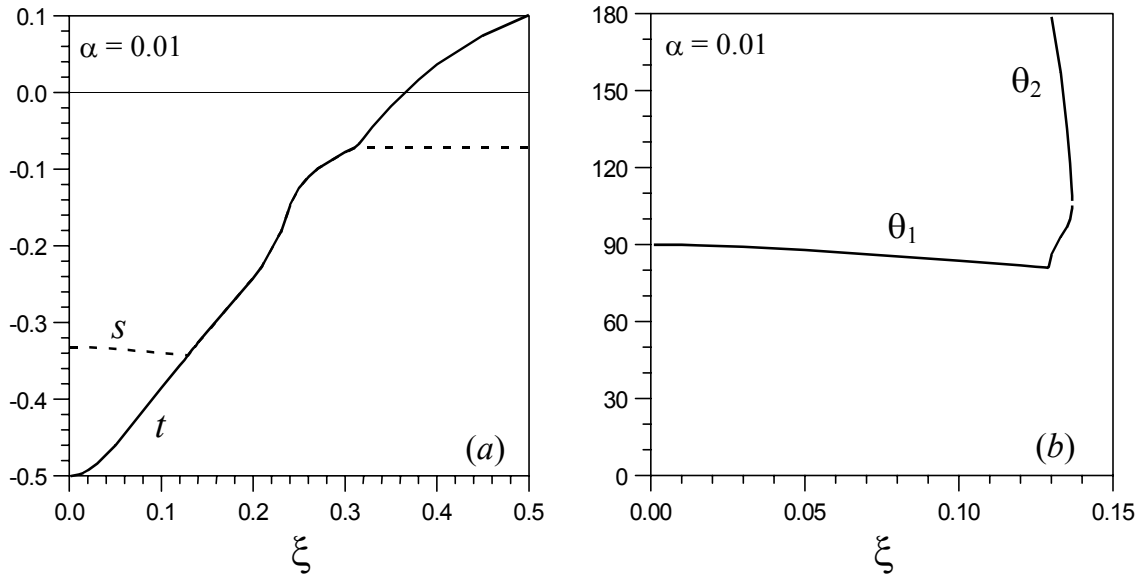


Figure 1: stress and couple stress singularities (a), elastic unloading and plastic reloading angles (b) as functions of the ratio  $\xi$ , under mode I for  $\nu = 0.3$  and  $\alpha = 0.01$ .

## MODE I AND MODE II PLANE STRAIN RESULTS

Values of the exponents  $s$  and  $t$ , elastic unloading and reloading angles  $\theta_1$  and  $\theta_2$  under mode I plane strain conditions are reported for various values of the characteristic lengths ratio  $\xi = l_e/l$  in Fig. 1, for  $\alpha = 0.01$  and  $\nu = 0.3$ . The stress singularity predicted by the classical  $J_2$ -flow theory for this value of  $\alpha$  results as being extremely weak, namely  $s = -0.0805$ , and the corresponding elastic unloading and plastic reloading angles are  $\theta_1 = 135.36$  and  $\theta_2 = 145.61$ , as may be found by following the approaches of Ponte Castañeda [4], or Bigoni and Radi [11] for vanishing pressure sensitivity. In Fig. 1a three distinct regions may be observed for increasing values of  $\xi$  between 0 and 0.5, where  $t < s$ ,  $t = s$  and  $t > s$ , respectively. Interestingly, as  $\xi$  tends to zero, namely for vanishing elastic characteristic length, the singularity of the couple stress fields  $t$  tends to the elastic singularity  $-0.5$ , whereas the singularity of the stress fields  $s$  approaches  $-0.33$ . Further investigations show that these limit values for  $t$  and  $s$  are found to be almost independent of the hardening coefficient  $\alpha$ . In any case, for  $\xi \ll 1$  the strength of the stress singularity increases with respect to the classical  $J_2$ -flow theory. For  $\xi < 0.13$  the couple stresses dominate the asymptotic solution and thus, the effective stress has the same singularity of the couple stress field within this range (eq. 19). However, as  $\xi$  approaches the value 0.13 from below, the exponent of the couple stress singularity  $t$  tends to increase and to coincide with the exponent of the stress singularity  $s$ . For  $0.13 \leq \xi \leq 0.31$  the negative exponents  $t$  and  $s$  are coincident and, thus, both stress and couple stress fields display the same singularity. As  $\xi$  increases, the strength of

singularity decreases and, for  $\xi = 0.31$ , the magnitude of the leading order term of the couple stress field  $\mathbf{m}$  tends to vanish. For  $\xi > 0.31$ , the solution is stress-dominated and the stress singularity assumes the value  $s = -0.071$  independently of  $\xi$ . This kind of solution for the leading order term of the stress field may be actually found for every value of the ratio  $\xi$ . For the stress-dominated solution, in fact, the ratio  $\xi$  has no influence on the stress field, but affects only the couple stress field, which appears to be not singular for  $\xi < 0.31$ . However, the stress dominated solution is not expected to recover the results obtained in [4] for the classical  $J_2$ -flow theory, as the leading order term of the velocity field turns out to be irrotational and a skew-symmetric stress component occurs for the present analysis.

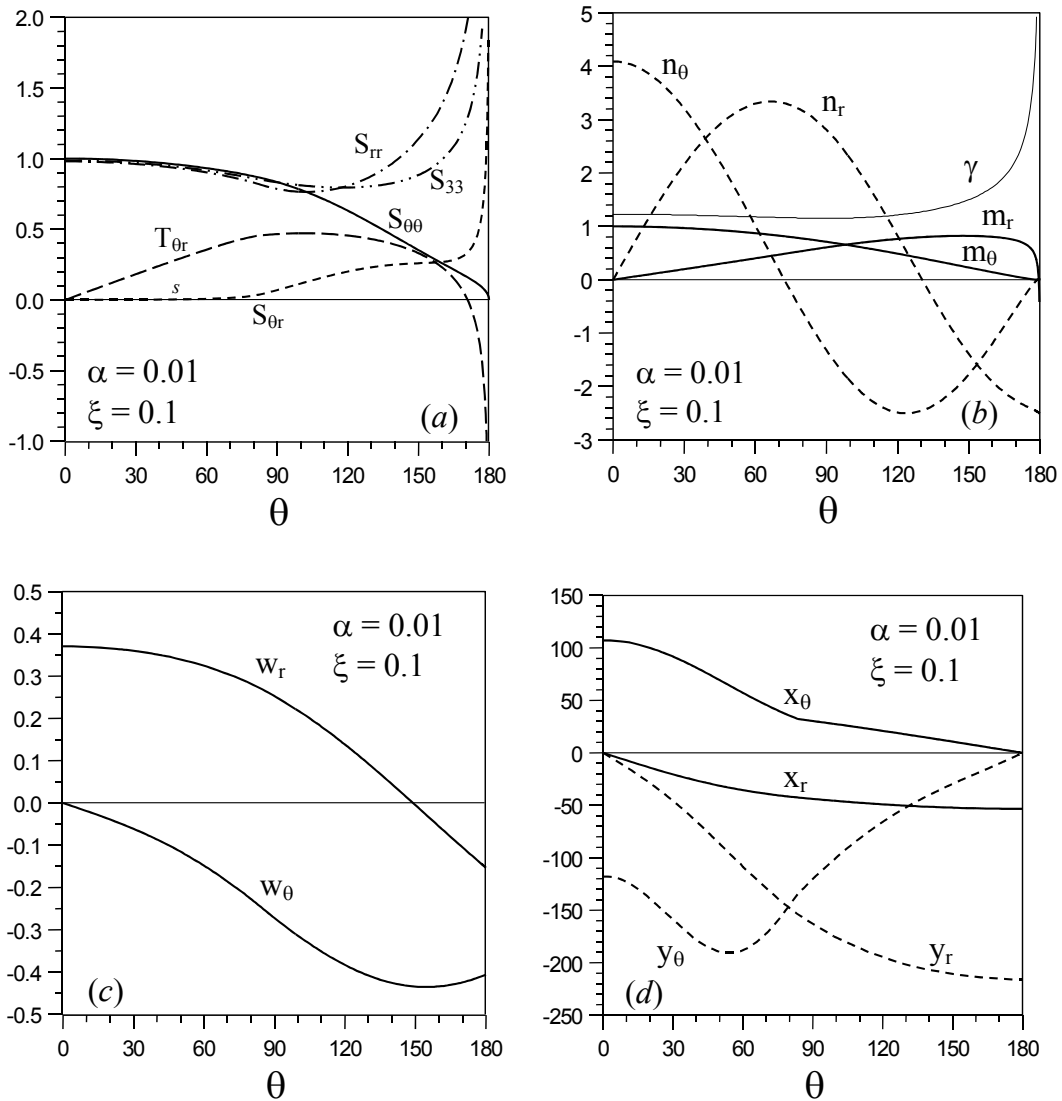


Figure 2: angular variations of the asymptotic fields of stress (a), couple stress (b), velocity (c) and deformation curvature rate (d) under mode I for  $\nu = 0.3$  and  $\alpha = 0.01$ .

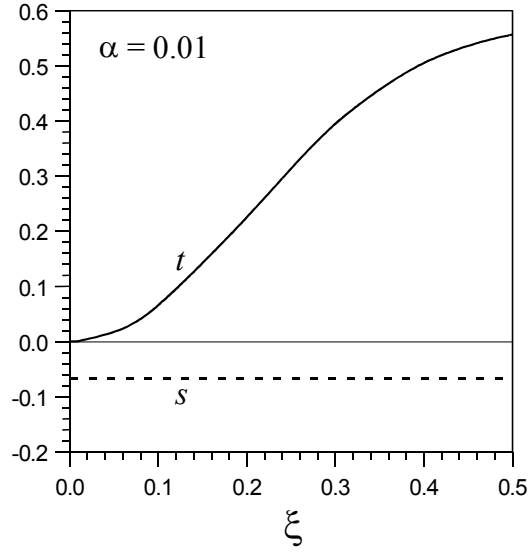


Figure 3: stress and couple stress singularities as functions of the ratio  $\xi$ , under mode II for  $\nu = 0.3$  and  $\alpha = 0.01$ .

The variation of the elastic unloading and reloading angles,  $\theta_1$  and  $\theta_2$ , with  $\xi$  is then reported in Fig. 1b, for  $\alpha = 0.01$ . As  $\xi$  tends to vanish, an elastic unloading sector starts at  $\theta_1 \approx \pi/2$  and extends up to the crack flanks. For  $\xi \geq 0.13$  a plastic reloading sector appears and the elastic unloading sector rapidly reduces in size and tends to vanish for  $\xi \cong 0.137$ . For  $\xi > 0.137$  the crack-tip zone is fully plastic, as already observed by Wei and Hutchinson [12] in their finite element investigations performed for  $\xi = 0.5$ .

As noted in [5] the considered constitutive model may give reasonable predictions for small values of  $\xi$ , namely  $\xi \ll 1$ , in view of the fact that the magnitude of the couple stress in the elastic sector results as being proportional to  $\xi$ . As the strain gradient effects are associated with the occurrence of dislocations, they scarcely influence the elastic behaviour. Therefore, the results obtained for small values of  $\xi$  are expected to be more realistic.

The angular distributions of the asymptotic crack-tip fields, normalized by conditions  $S_{\theta\theta}(0) = 1$  and  $m_{\theta}(0) = 1$ , are plotted in Fig. 2, for  $\xi = 0.1$  and  $\alpha = 0.01$ . In particular, Fig. 2a shows that the tensile stress field ahead of the crack-tip is characterized by large stress triaxiality and the symmetric part of the shear stress, namely  $S_{r\theta}$ , is almost vanishing within the plastic loading sector. Moreover,  $S_{\theta r}$  and  $T_{\theta r}$  tend to opposite values on the crack faces, as required by the boundary condition  $(3)_1$ . Fig. 2b shows the angular variation of the couple stress fields  $\mathbf{m}$  and  $\mathbf{n}$  and that of the current flow stress  $\gamma$ . Note that the current flow stress, which is given by the single contribution from the couple stress field as  $t < s$ , seems to be almost constant within the plastic loading sector and tends to diverge at the crack flanks as is usual for crack propagation problems in elastic-plastic materials displaying linear isotropic hardening.

The angular variations of the velocities and deformation curvature rates are shown in Figs. 2c, d. It may be observed that the velocity component  $w_{\theta}$  at  $\theta = \pi$  is negative, thus implying crack-tip opening. Moreover, the deformation curvature rates are also present in the elastic unloading sector, although  $x_{\theta}$  assumes larger values within the plastic loading sector ahead of the crack-tip.



The variations of  $s$  and  $t$  with the characteristic lengths ratio  $\xi$  under mode II loading conditions are reported in Fig. 3, for  $\alpha = 0.01$ . From these findings it appears that the exponent  $t$  of the couple stress field vanishes as  $\xi$  tends to zero and tends to increase for  $\xi > 0$ . Therefore, mode II crack propagation does not result in singular couple stresses, as already observed for a stationary crack in strain gradient [9]. It follows that the asymptotic fields are stress-dominated and, thus, the leading order terms of the stress and velocity fields do not depend on the value of  $\xi$ . In particular, the stress singularity  $s = -0.0659$  has been detected for every value of  $\xi$ , together with a fully plastic crack-tip zone with no elastic unloading sector.

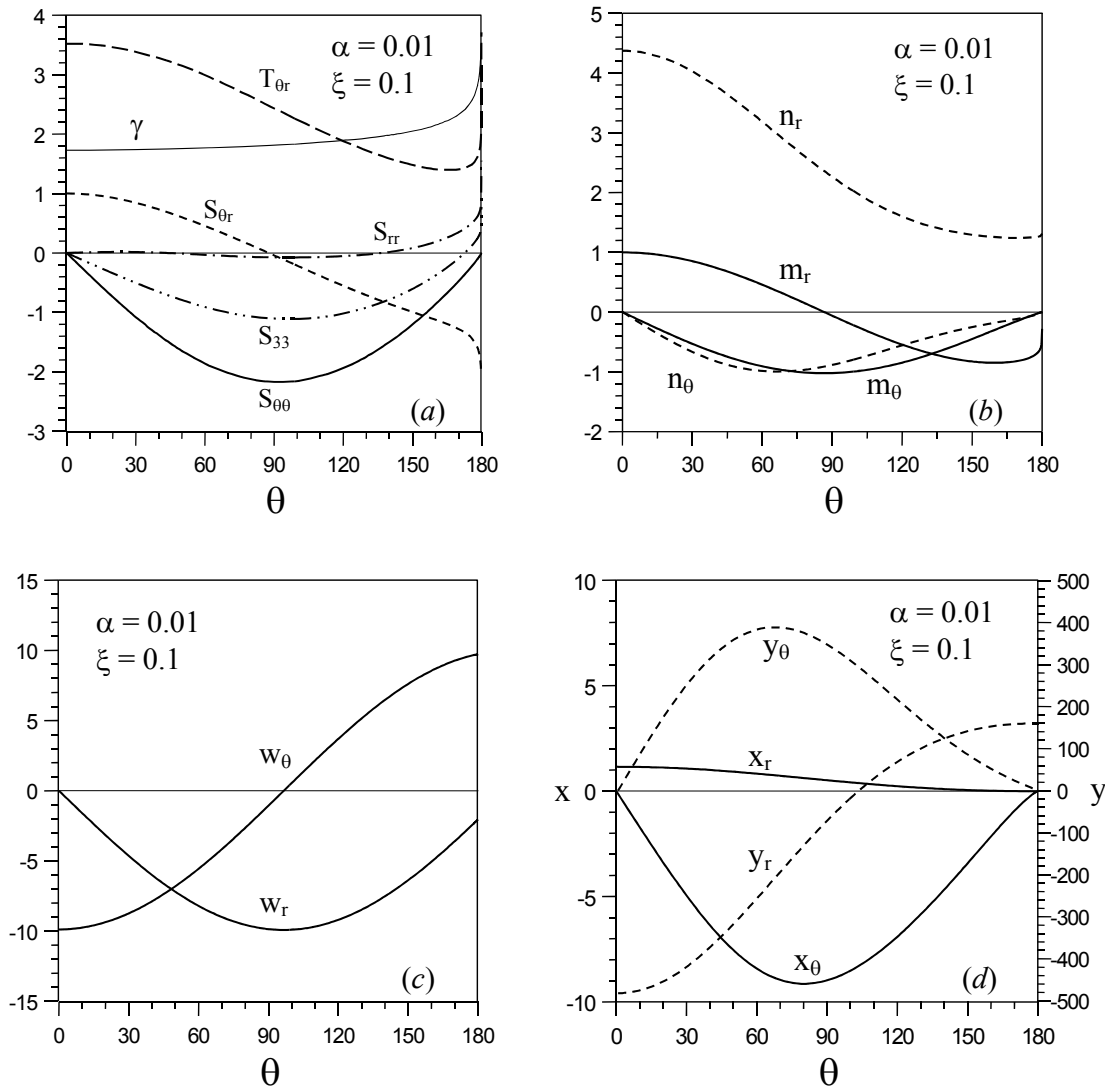


Figure 4: angular variations of the asymptotic fields of stress (a), couple stress (b), velocity (c) and deformation curvature rate (d) under mode II for  $\nu = 0.3$  and  $\alpha = 0.01$ .

The angular variations of stress, couple stress, velocity and deformation curvature rate functions for mode II crack propagation, normalized by conditions  $S_{\theta r}(0) = 1$  and  $m_r(0)$

$= 1$ , are plotted in Fig. 4 for  $\xi = 0.1$  and  $\alpha = 0.01$ . From Fig. 4a it can be observed that the skew-symmetric shear stress  $T_{\theta r}$  largely exceeds the symmetric component  $S_{\theta r}$  and the current flow stress  $\gamma$  ahead of the crack-tip. Therein, the shear traction, which is given by the sum of  $S_{\theta r}(0)$  and  $T_{\theta r}(0)$ , is almost equal to 2.6 times the magnitude of the current flow stress  $\gamma(0)$  and, thus, appears to be larger than in classical plasticity due to the contribution from the anti-symmetric shear stress. As the mode II solution is stress dominated the current flow stress is given by the single contribution from the symmetric stress field. The elastic characteristic length influences only the couple stress and deformation curvature rate functions, even if their qualitative trend undergoes little change with  $\xi$ . Note also that two different scales have been adopted in Fig. 4d for the leading order and the higher order terms, namely  $\mathbf{x}$  and  $\mathbf{y}$ .

## REFERENCES

1. Hutchinson J.W., “*Plasticity at the micron scale*”, Int. J. Solids Struct. 2000, **37** 225-238.
2. Elssner G., Korn D., Rühle M., “*The influence of interface impurities on fracture energy of UHV diffusion bonded metal-ceramic bicrystals*”, Scripta Metall. Mater. 1994, **31** 1037-1042.
3. Drugan W.J., Rice J.R., Sham, T.L., “*Asymptotic analysis of growing plane strain tensile cracks in elastic-ideally plastic solids*”, J. Mech. Phys. Solids 1982, **30** 447-473.
4. Ponte Castañeda P., “*Asymptotic fields in steady crack growth with linear strain-hardening*”, J. Mech. Phys. Solids 1987, **35** 227-268.
5. Fleck N.A., Hutchinson J.W., “*A phenomenological theory for strain gradient effects in plasticity*”. J. Mech. Phys. Solids 1993, **41** 1825-1857.
6. Toupin R.A., “*Elastic materials with couple-stresses*”, Arch. Rat. Mech. Anal. 1962, **11** 385-414.
7. Mindlin R.D., Tiersten H.F., “*Effects of couple-stresses in linear elasticity*”, Arch. Rat. Mech. Anal. 1962, **11** 415-448.
8. Xia Z.C., Hutchinson J.W., “*Crack-tip fields in strain gradient plasticity*”, J. Mech. Phys. Solids 1996, **44** 1621-1648.
9. Huang Y., Zhang L., Guo T. F., Hwang K.C., “*Mixed mode near-tip fields for crack in materials with strain-gradient effects*”, J. Mech. Phys. Solids 1997, **45** 439-465.
10. Radi E., “*Strain-gradient effects on steady-state crack growth in linear hardening materials*”, J. Mech. Phys. Solids, in press.
11. Bigoni D., Radi E., “*Mode I crack propagation in elastoplastic pressure-sensitive materials*”, Int. J. Solids Struct. 1993, **30** 899-919.
12. Wei Y., Hutchinson J.W., “*Steady-state crack growth and work of fracture for solids characterized by strain gradient plasticity*”, J. Mech. Phys. Solids 1997, **45** 1253-1273.